Biomedical Engineering Letters (2022) 12:197–203
https://doi.org/10.1007/s13534-022-00219-x

ORIGINAL ARTICLE

# Rapid and low-cost, and disposable electrical sensor using an extended gate field-effect transistor for cardiac troponin I detection

Kang Hyeon Kim[1] · Kyung Wook Wee[1] · CheonJung Kim[1] · Don Hur[1] · Jeong Hoon Lee[1] · Yong Kyoung Yoo[2]

Received: 27 December 2021 / Revised: 17 January 2022 / Accepted: 26 January 2022 / Published online: 8 February 2022


**Abstract**
Field effect transistor (FET) biosensor is based on metal oxide field effect transistor that is gated by changes in the surface charges induced the reaction of biomolecules. In most cases of FET biosensor, FET biosensor is not being reused after the reaction; therefore, it is an important concept of investigate the biosensor with simplicity, cheap and reusability. However, the conventional cardiac troponin I (cTnI) sensing technique is inadequate owing to its low sensitivity and high operational time and cost. In this study, we developed a rapid and low-cost, and disposable electrical sensor using an extended gate field-effect transistor (EGFET) to detect cTnI, as a key biomarker for myocardiac infarction. We first investigated pH sensing characteristics according to the pH level, which provided a logarithmically linear sensitivity in the pH sensing buffer solution of approximately 57.9 mV/pH. Subsequently, we prepared a cTnI sample and monitored the reaction between cTnI and cTnI antibodies through the changes in the drain current and transfer curves. Our results showed that the EGFET biosensor could successfully detect the cTnI levels as well as the pH with low-cost and rapid detection.

## 1 Introduction

Cardiovascular diseases (CVD), a group of afflictions affecting the heart and blood vessels, are the most common cause of death globally. According to the World Health Organization (WHO), 17.9 million reported deaths were due to CVD, accounting for 32% of global deaths [1]. Mortality due to CVD is expected to reach 23.3 million in 2030, resulting in enormous social loss. Acute myocardial infarction is the result of myocardial necrosis caused when an occlusive thrombus blocks coronary arteries. It is prevalent and potentially fatal [2–4]. In most cases of acute myocardial infarction, the indicators of the disease are not easily recognizable [5–7]. Therefore, rapid and accurate diagnosis is crucial when an infarction occurs. When the coronary artery is completely blocked, myocardial damage can be prevented if treated within 2 h and complications avoided if treated within 12 h [8, 9]. Since the symptoms of myocardial infarction are atypical[5], diagnosis requires an additional test before medical treatment. Electrocardiography (ECG) is the most common diagnostic method for myocardial infarction [10], but only 57% of affected patients are diagnosed with acute myocardial infarction using this method. Thus, a body-fluid-based component analysis sensing system is required for rapid and accurate confirmation [11, 12].

The myocardium, present solely in the heart, comprises muscle enzymes, such as aspartate aminotransferase (AST), lactate dehydrogenase (LDH), and creatine phosphokinase (CPK), and proteins, such as cardiac troponin I (cTnI) and cardiac troponin T (cTnT) [13–15]. These enzymes and proteins are released into the bloodstream when myocardial necrosis occurs due to acute myocardial infarction, resulting in a change in their concentrations in the blood [13, 14]. A higher degree of necrosis in the myocardium results in a higher number of

Kang Hyeon Kim and Kyung Wook Wee have equally contributed to this study.

✉ Don Hur
dhur@kw.ac.kr

✉ Jeong Hoon Lee
jhlee@kw.ac.kr

✉ Yong Kyoung Yoo
yongkyoung0108@cku.ac.kr

[1] Department of Electrical Engineering, Kwangwoon University, 20 Kwangwoon-ro, Nowon-gu, Seoul 01897, South Korea

[2] Department of Electonic Engineering, Catholic Kwandong University, 24, Beomil-ro 579beon gil, Gangneung-si, Gangwond-do 25601, South Korea

enzymes and proteins in the blood. In addition, cTnI and TnT, which have high specificity and sensitivity, are absent in the other organs. Therefore, they can be used as biomarkers for acute myocardial infarction [15, 16]. Typically, for the actual detection of cTnI and cTnT, a lateral flow assay with colorimetric nanoparticles and an enzyme-linked immunosorbent assay with fluorescence dyes are employed. However, the limitations of cTnI sensing, such as the long operation time, low sensitivity, and expensive equipment, need to be addressed.

In particular, the biomarkers with the blood concentrations in the range of 0.0–0.3 ng/mL necessitate analytical techniques that are simple, quick, highly sensitive, and inexpensive [17, 18]. Therefore, many research groups have investigated solid-state biosensors with metal-oxide-semiconductor field-effect transistors (MOSFET) [19–21], which possess several advantages, such as low cost and highly sensitive output. An ion-sensitive field-effect transistor (ISFET) sensor [22–24], which uses the field effect of ions and biomolecules, comprises a reference electrode and a recognition material with a field-effect transistor (FET). The reaction between the analyte and the recognition material causes the drain-source current ($I_{DS}$) induced by the gate voltage ($V_G$) to vary with the field effect of the reaction. Conventional FET-based biosensors have a highly sensitive output and selectivity; however, they have limited reusability owing to their integration with the recognition layer. Moreover, the effects of noise should be addressed because the gate of the conventional FET biosensor is directly exposed to the sample solution.

In this study, we developed a biosensor with an extended gate field-effect transistor (EGFET) for the direct electrical detection of cTnI. The EGFET sensor comprises a conventional FET, sensing pad, and microfluidic channel chip. We used a commercialized FET connected to an extended gate and a titanium oxide ($TiO_2$) surface, which acts as an easily replaceable sensing layer. To test the change in electrical signals caused by the field-effect of ion charges, we first monitored the $I_{DS}$ change corresponding to the $H^+$ ion concentration under various pH conditions in buffer solutions. Finally, to demonstrate the ability of the immunoassay, we immobilized the cTnI antibody on the Au sensing layer and monitored the electrical signal changes from the cTnI antigen–antibody reaction. Furthermore, we discuss the performance of the proposed extended FET biosensor from the perspective of the clinical range of cTnI.

## 2 Materials and methods

### 2.1 Device and measurement system setup

A Si-based external gate was designed for the EGFET sensing pad. First, a sensing pad was fabricated with eight parallel channels using microfabrication, as illustrated in Fig. 1a. Subsequently, the sensing pad was functionalized with a cTnI antibody to selectively detect cTnI molecules. After antibody immobilization, a polydimethylsiloxane (PDMS) microfluidic channel chip was assembled on the sensing pad. Figure 1a illustrates the setup of the electrical measurement system. Each sensing pad was connected with the commercialized metal oxide FET (Texas Instruments n-MOSFET CD4007UBE) as shown in Fig. 1a and b. The pH and cTnI sensing properties including sensitivity, linearity, and transfer curves were measured in the sample solutions through Ag/AgCl reference electrodes using a parameter analyzer (Keithley 4200-SCS) with source measurement units. The commercialized MOSFET with the gate length and width of 10 and 30 µm, respectively, was used as an FET in our systems. These were connected to the parameter analyzer, drain, gate, and source parts of the FET using a coaxial cable. Finally, the electrical signals from the sample reaction were measured using a PDMS microfluidic channel, as shown in Fig. 1c.

### 2.2 Device fabrication

As shown in Fig. 2a, first, a silicon substrate was prepared after cleaning. A layer of silicon dioxide ($SiO_2$) with a thickness of 300 nm was deposited for insulation using plasma-enhanced chemical vapor deposition (PECVD). To form electrodes, Au and Cr layers with thicknesses of 100 and 30 nm were deposited on the $SiO_2$ layer. The Cr layer was adopted as an adhesion layer between the Au and $SiO_2$ layers. After depositing the Au layer, the electrodes were patterned using photolithography (MA6 Aligner, Karl Suss) and Au lift-off (e-beam evaporator). Titanium oxide as a sensing layer of EGFET with 30 nm thickness was deposited using PECVD. Finally, a PDMS microfluidic channel with a width of 1 mm and a thickness of 50 µm was designed to deliver test samples and induce biological reactions between target biomolecules and their antibodies through microchannels.

### 2.3 Antibody immobilization and cardiac troponin I reaction

After preparing the external gate for the sensing pad of the EGFET via microfabrication, the $TiO_2$ surface of the sensing pad was cleaned using a piranha solution (4:1 ratio of $H_2SO_4$ (98.08%) and $H_2O_2$ (34.01%)) for 30 min to remove any contaminants and then rinsed with deionized water as shown in Fig. 2b. Subsequently, to form the amine group, a 2 wt% (3-aminopropyl)triethoxysilane (APTES, Sigma-Aldrich) solution in ethanol was prepared, with which the sensing pad was treated for 3 h [25]. Thereafter, a 1% glutaraldehyde solution was used to form a layer of antibody linkers on the pad. After aldehyde-group formation,

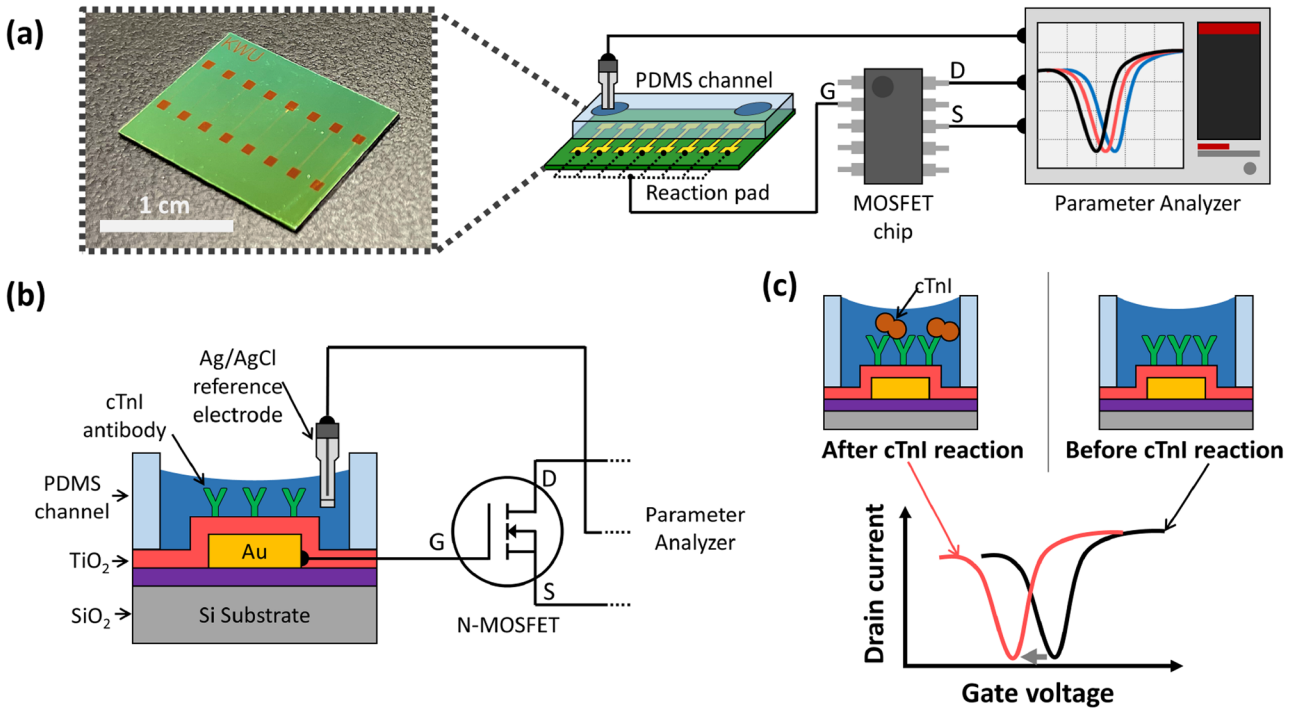


**Fig. 1** **a** Schematic of the EGFET with sensing pad and measurement setup. This comprises an electrical measuring system (parameter analyzer), conventional MOSFET, and a sensing pad with a reference electrode. **b** Schematic of the basic cross-section of EGFET. **c** Sensing mechanism for shift transfer curves by interaction between cTnI and antibody

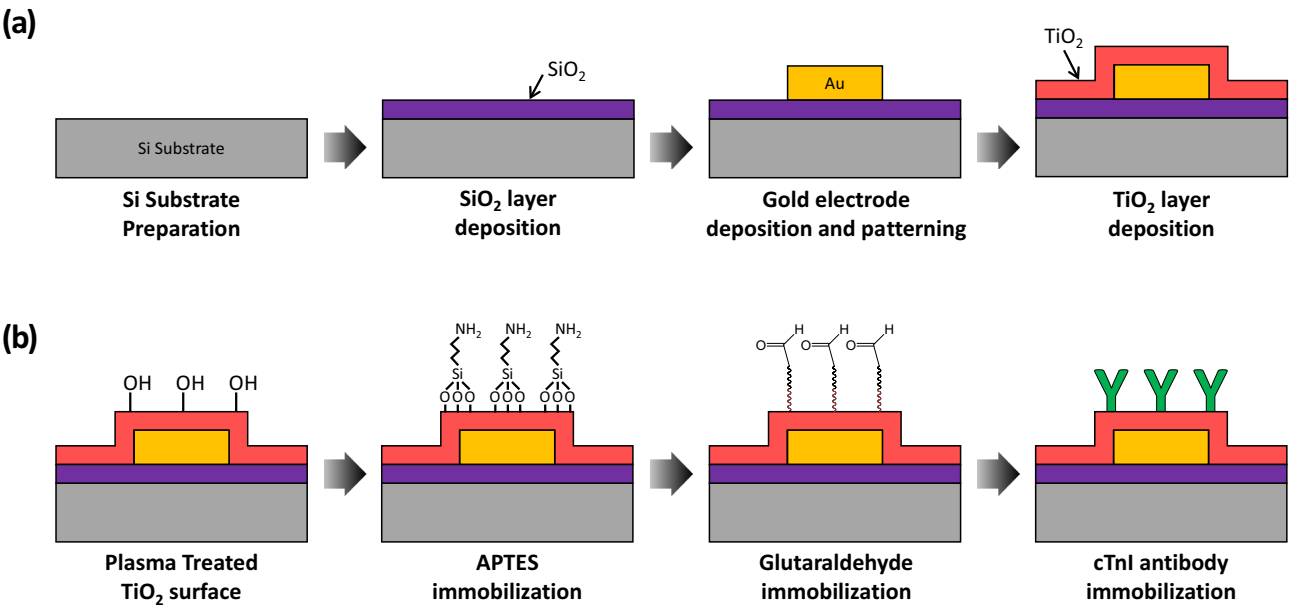


**Fig. 2** Illustration of **a** sensing pad fabrication with micromachining and **b** antibody functionalization process

the reaction pad was immersed in a 10 µg/mL cardiac TnI monoclonal antibody (19C7; Thermo Fisher Scientific) in a 1X phosphate-buffered saline for 2 h. For cTnI and its antibody reaction, cardiac cTnI (Sigma-Aldrich) in 1X PBS was prepared to obtain a target concentration of 0.01–100 ng/mL. The diluted cTnI sample was injected into the sensing pad and allowed to react for 20 min.

Finally, the external gate for the sensing pad was washed with a 1X PBS buffer after the cTnI reaction.

## 3 Results and disscussion

### 3.1 pH sensing characterization

Prior to performing cTnI detection with the fabricated EGFET biosensor, we first examined its pH sensing performance using solutions of different pH. We prepared various pH buffer solutions (pH levels in the range of 4–10) and sequentially injected each of them into the PDMS microfluidic channel. We monitored the changes in the $V_G$-induced drain current caused by the field-effect of the $H^+$ ion concentration using a parameter analyzer. Depending on the pH level, the transfer curves of EGFET shifted (dashed line, as shown in Fig. 3). The relationship between the gate voltage ($\Delta V_G$) and pH can be represented as follows [26]:

$$\Delta V_G = 2.3\frac{kT}{q}\alpha\Delta pH$$

where k represents the Boltzmann constant, T represents the temperature, q is the electrical charge of the $H^+$ ion, and α represents the sensitivity factor. Ideally, the theoretical sensitivity is 59 mV/pH with a = 1 at room temperature. In this regard, $\Delta V_G$ depends on the pH conditions caused by the protonation and deprotonation of the EGFET sensing pad. In Fig. 3, the transfer curves are shifted toward the right according to the pH conditions, while the shape of the transfer curve remained unchanged. We estimated the logarithmic linear sensitivity of $V_G$ according to various pH levels (pH 3–10), as shown in inset graph of Fig. 3. The result reveals that the sensors exhibit excellent linearity ($R^2 = 0.9923$) with a steep slope of approximately 57.9 mV/pH at $I_{DS} = 4$ μA. To evaluate whether the measurement is reliable, we performed a repeatability test in which both buffer solutions of pH 10 and 6 were injected through the microchannel repeatedly. Figure 4 shows the results in which repeated output signals at each pH level are similar. This implies that our extended FET biosensors possess good repeatability.

### 3.2 Quantification of troponin I

We demonstrated the relationship between $I_{DS}$ and $V_G$ at five different cTnI concentrations using the EGFET biosensor. First, we used a syringe pump to drive the samples or buffer solutions through the microchannel. PBS solutions were used for control experiments. Subsequently, we monitored various concentrations of cTnI samples ranging from 0.01 to 100 ng/mL. Twenty minutes after initiation, we injected the PBS buffer solution to wash out non-reacted cTnI samples and then measured $I_{DS}$ with $V_G$. As shown in Fig. 5, we clearly observed that the transfer curves were shifted by the cTnI -anti-cTnI interactions. Interestingly, the curves shifted as the concentration of cTnI increased, while the shape and magnitude of the transfer curves remained unchanged (see arrow in Fig. 5). This invariability of the shape and magnitude provides an additional strong advantage. The $V_G$ shift at

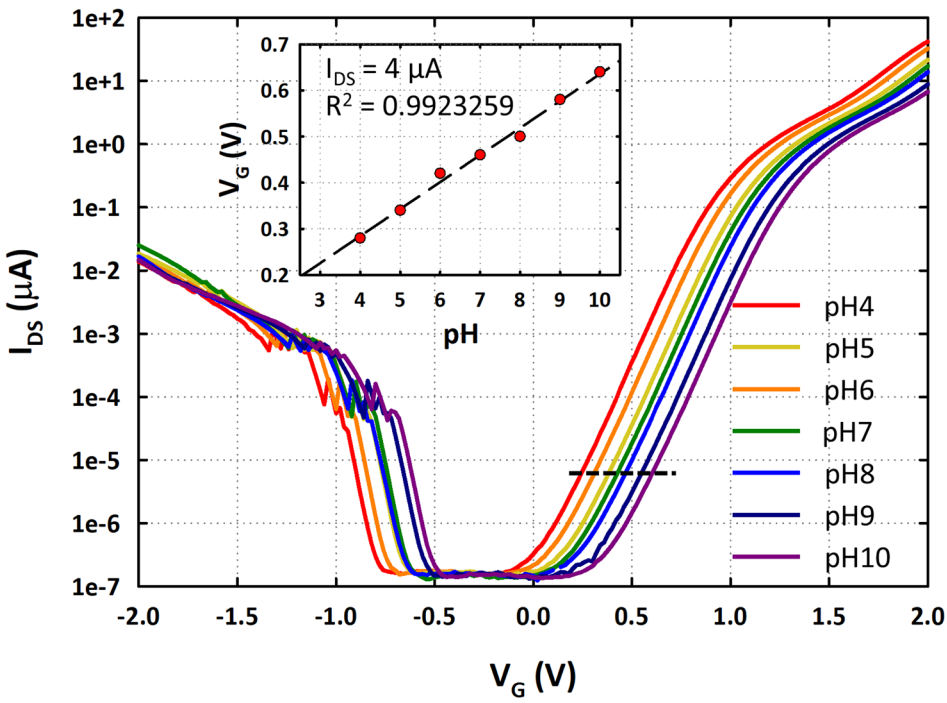


**Fig. 3** EGFET pH sensing characteristics. The inset graph illustrates that changes in the drain current according to pH levels

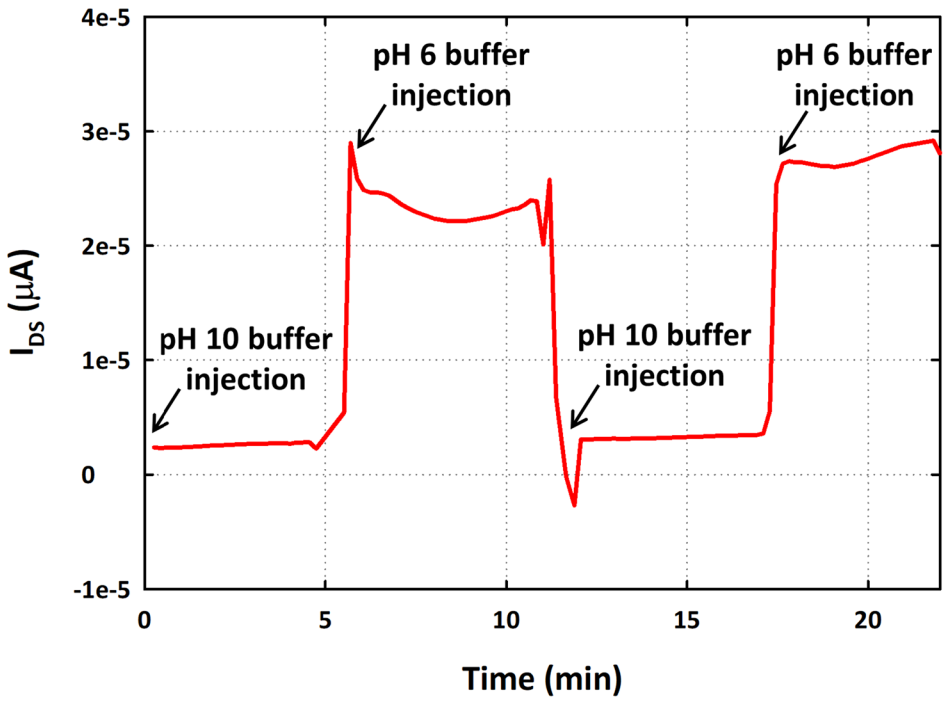


**Fig. 4** Repeatability test of EGFET using the current measurements ($I_{DS}$) from the sequential injections of different pH (pH10 and pH6)

a constant $I_{DS}$ is purely attributed to the change in biological environment because of the invariability, which is indicative of the reliable operation of our sensors.

In Fig. 6, we assessed the logarithmic linear sensitivity at five different cTnI sample concentrations for $I_{DS} = 10$ μA. We repeated the experiment by performing five independent runs using multiple EGFET biosensors. We analyzed the data using logarithmically linear fitting. The results reveal that our sensors exhibit excellent linearity ($R^2 > 0.94$) with a steep slope of 3.42535. We believe that good linearity is advantageous for reliable detection of cTnI. From these results, the clinical range of normal cTnI levels has been reported as 0.0–0.04 ng/mL. The clinical cutoff level of cTnI in blood was reported as 0.1 ng/mL [27]. our egFET sensors

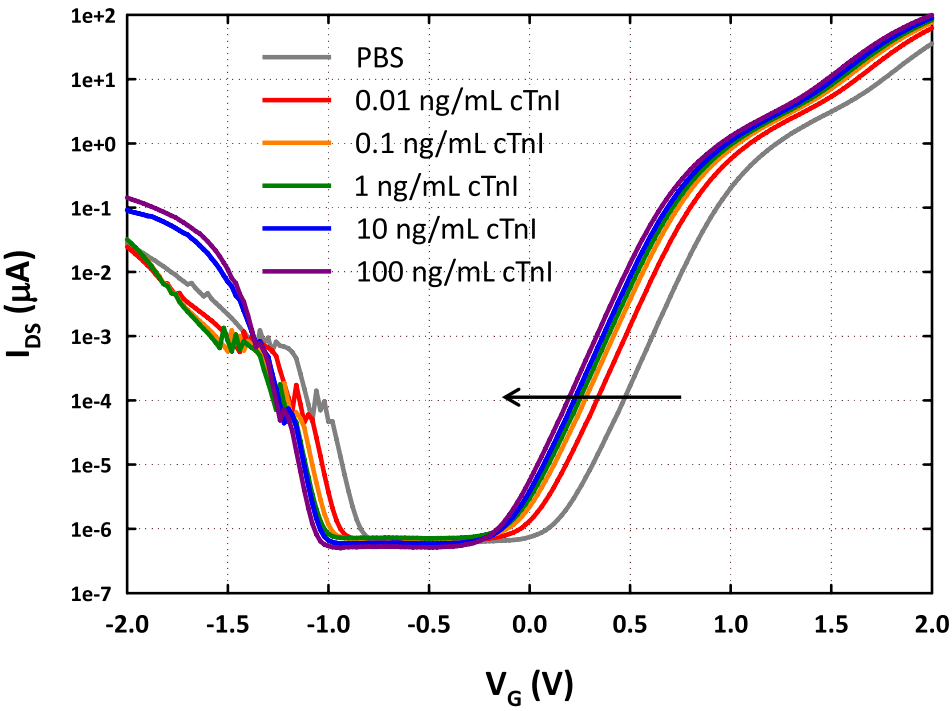


**Fig. 5** EGFET cTnI sensing characteristics. The shift in the transfer curves according to the cTnI concentration is depicted using the arrow

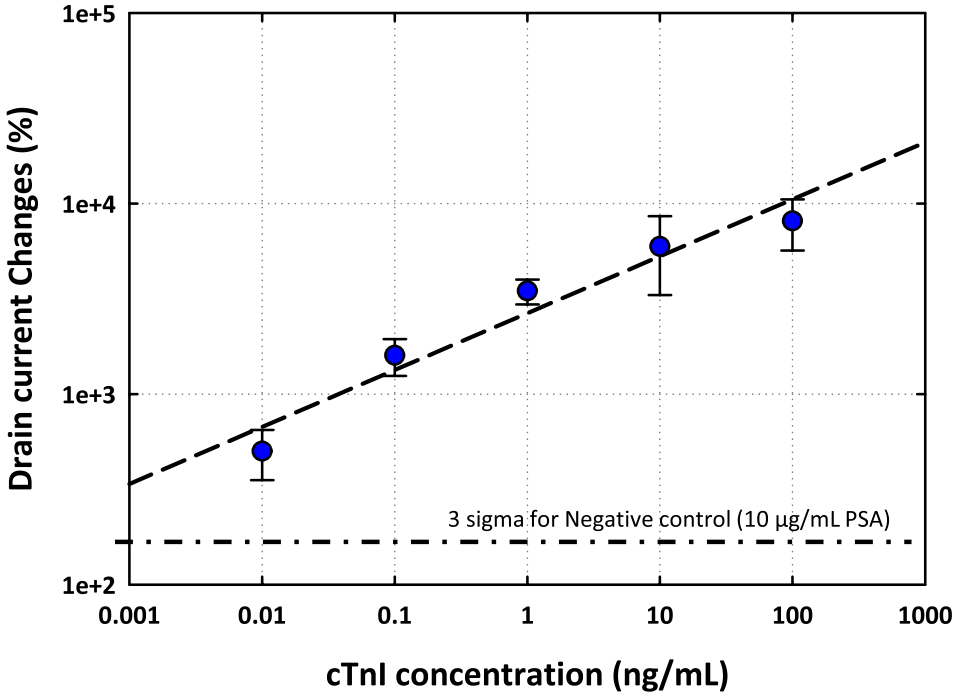


**Fig. 6** cTnI detection test was based on logarithmically linear sensitivity against various cTnI concentrations. The selectivity test compared the detection of 10 µg/mL PSA and 0.01 ng/mL cTnI concentrations

exhibit an excellent linearity ($R^2 > 0.94$) with good sensitivity to detect cTnI levels clinically.

To test selectivity, we injected a 10 µg/mL prostate cancer antigen into the PDMS microfluidic channel and monitored the drain current according to the same protocol described for cTnI. As shown in the negative control line in Fig. 6, we observed large drain current changes at 0.01 ng/mL cTnI concentrations while no significant changes occurred in the drain current at a considerably higher concentration of 10 µg/mL PSA. The limit of detection (LOD) was estimated to be below 1 pg/ml cTnI. Finally, we conclude that our extended FET biosensors possess excellent re-usability and outstanding performance of good linearity and extremely low LOD.

## 4 Conclusion

In summary, we investigated a rapid and low-cost highly sensitive EGFET biosensor for detecting cTnI. We designed a Si-based external gate for the sensing pad of the EGFET and directly monitored electrical signals using a commercialized n-MOSFET. To demonstrate the ability of the developed EGFET to sense the required biomarkers, we first examined its performance under different pH conditions. The results revealed a high sensitivity of approximately 57.9 mV/pH. Subsequently, to investigate the ability of the immunoassay, we monitored the changes in the drain current for different cTnI concentrations. The results again revealed a good sensitivity with good selectivity based on a Si-based external gate with a commercialized FET. Thus, we believe that our EGFET platform offers new opportunities and benefits for simple and cheap electrical detection with a low cost (commercial FET chip approximately 70 cents for Texas Instruments n-MOSFET CD4007UBE), and reusability (reuse of FET sensor), and direct detection for POCT.

**Acknowledgements** This work was supported by the National Research Foundation of Korea (NRF, grant no. NRF-2020R1G1A1102736). Also, D. Hur was supported by a research grant from Kwangwoon University in 2022.

**Funding** The authors have not disclosed any funding.

## Declarations

**Conflict of interest** The authors declare no competing financial interests.

## References

1. WHO: Cardiovascular diseases (CVDs). from https://www.who.int/en/news-room/fact-sheets/detail/cardiovascular-diseases-(cvds)
2. White HD, Chew DP. Acute myocardial infarction. The Lancet. 2008;372:570–84.
3. Anderson JL, Morrow DA. Acute myocardial infarction. N Engl J Med. 2017;376:2053–64.
4. Mattila KJ, Nieminen MS, Valtonen VV, et al. Association between dental health and acute myocardial infarction. BMJ. 1989;298:779.

5. Goldberg RJ, Yarzebski J, Lessard D, Gore JM. Decade-long trends and factors associated with time to hospital presentation in patients with acute myocardial infarction: the worcester heart attack study. Arch Intern Med. 2000;160:3217–23.
6. Goldberg RJ, Brady P, Muller JE, et al. Time of onset of symptoms of acute myocardial infarction. Am J Cardiol. 1990;66:140–4.
7. Moser DK, McKinley S, Dracup K, Chung ML. Gender differences in reasons patients delay in seeking treatment for acute myocardial infarction symptoms. Patient Educ Couns. 2005;56:45–54.
8. Lindahl B, Toss H, Siegbahn A, Venge P, Wallentin L. Markers of myocardial damage and inflammation in relation to long-term mortality in unstable coronary artery disease. N Engl J Med. 2000;343:1139–47.
9. Bradley EH, Herrin J, Wang Y, et al. Strategies for reducing the door-to-balloon time in acute myocardial infarction. N Engl J Med. 2006;355:2308–20.
10. Trägårdh E, Claesson M, Wagner GS, Zhou S, Pahlm O. Detection of acute myocardial infarction using the 12-lead ECG plus inverted leads versus the 16-lead ECG (with additional posterior and right-sided chest electrodes). Clin Physiol Funct Imaging. 2007;27:368–74.
11. Labugger R, Organ L, Collier C, Atar D, Van Eyk JE. Extensive troponin I and T modification detected in serum from patients with acute myocardial infarction. Circulation. 2000;102:1221–6.
12. Kristono GA, Holley AS, Hally KE, et al.: An IL-6-IL-8 score derived from principal component analysis is predictive of adverse outcome in acute myocardial infarction, Cytokine: X, 2020, 2: 100037.
13. Franken NAP, Strootman E, Hollaar L, van der Laarse A, Wondergem J. Myocardial enzyme activities in plasma after whole-heart irradiation in rats. J Cancer Res Clin Oncol. 2000;126:27–32.
14. Roongsritong C, Warraich I, Bradley C. Common causes of troponin elevations in the absence of acute myocardial infarction: incidence and clinical significance. Chest. 2004;125:1877–84.
15. Cullen L, Parsonage WA, Greenslade J, et al. Delta troponin for the early diagnosis of AMI in emergency patients with chest pain. Int J Cardiol. 2013;168:2602–8.
16. Anders B, Alonso A, Artemis D, et al. What does elevated high-sensitive troponin I in stroke patients mean: concomitant acute myocardial infarction or a marker for high-risk patients. Cerebrovasc Dis. 2013;36:211–7.
17. Antman EM, Tanasijevic MJ, Thompson B, et al. Cardiac-specific troponin I levels to predict the risk of mortality in patients with acute coronary syndromes. N Engl J Med. 1996;335:1342–9.
18. Aviles RJ, Askari AT, Lindahl B, et al. Troponin T levels in patients with acute coronary syndromes, with or without renal dysfunction. N Engl J Med. 2002;346:2047–52.
19. Chae M-S, Yoo YK, Kim J, Kim TG, Hwang KS. Graphene-based enzyme-modified field-effect transistor biosensor for monitoring drug effects in Alzheimer's disease treatment. Sens Actuators, B Chem. 2018;272:448–58.
20. Chen C-P, Ganguly A, Lu C-Y, et al. Ultrasensitive in situ label-free DNA detection using a gan nanowire-based extended-gate field-effect-transistor sensor. Anal Chem. 2011;83:1938–43.
21. Lin T-W, Hsieh P-J, Lin C-L, et al. Label-free detection of protein-protein interactions using a calmodulin-modified nanowire transistor. Proc Natl Acad Sci. 2010;107:1047.
22. Sinha S, Pal T, Kumar D, et al. Design, fabrication and characterization of TiN sensing film-based ISFET pH sensor. Mater Lett. 2021;304:130556.
23. Zhao S, Shi C, Hu H, et al. ISFET and Dex-AgNPs based portable sensor for reusable and real-time determinations of concanavalin a and glucose on smartphone. Biosens Bioelectron. 2020;151:111962.
24. Chae M-S, Park JH, Son HW, Hwang KS, Kim TG. IGZO-based electrolyte-gated field-effect transistor for in situ biological sensing platform. Sens Actuators, B Chem. 2018;262:876–83.
25. Kim W-J, Kim S, Lee BS, et al. Enhanced protein immobilization efficiency on a TiO2 surface modified with a hydroxyl functional group. Langmuir. 2009;25:11692–7.
26. Bergveld P. Thirty years of ISFETOLOGY: what happened in the past 30 years and what may happen in the next 30 years. Sens Actuators, B Chem. 2003;88:1–20.
27. Mahajan VS, Jarolim P. How to interpret elevated cardiac troponin levels. Circulation. 2011;124:2350–4.